Spherical Multiple-Cell Grid in WAVEWATCH III

Jian-Guo Li*
Met Office, Exeter EX1 3PB, United Kingdom
12 October 2016

Contents

Corresponding author address: Dr Jian-Guo Li, Met Office, FitzRoy Road, Exeter EX1 3PB, UK
Email: Jian-Guo.Li@metoffice.gov.uk *Tel.* +44 1392 884885 *Fax*. +44 1392 885681.

1. Introduction

The ice edge in the Arctic is retreating at unexpected speeds in recent years and reached as high as 86^o N in summer 2007, opening new shipping routes cross the Arctic and calling ocean surface wave models to extend at high latitudes. The major problem to extend a latitude-longitude (lat-lon) grid wave model at high latitudes is the diminishing longitude grid-length towards the Pole, which exerts a severe restriction on time steps of finite-difference schemes (advection and diffusion in particular). Another problem is the increased curvature of the parallels at high latitudes. The rapid change of the local east direction renders the scalar assumption invalid for any vector component defined relative to the local east direction. The spherical multiple-cell (SMC) grid has been developed to tackle the polar problems (Li 2011). The SMC grid has the flexibility to remove all land points out of the wave propagation schemes and requires minimal changes to the lat-lon grid finite-difference schemes because the lat-lon "rectangular" cells are retained.

The SMC grid relaxes the Courant-Friedrichs-Lewy (CFL) restriction of the Eulerian advection time-step by merging longitudinal cells towards the Poles as in the reduced grid (Rasch 1994). Round polar cells are introduced to remove the polar singularity of the spherical coordinate system. Vector component propagation errors caused by the scalar assumption at high latitude is removed by replacing the local east with a fixed reference direction, for instance, the map-east as viewed in a polar stereographic projection, to define the wave spectral components in the Arctic.

Besides, unresolved small islands are incurring errors in global ocean surface wave models as they are important sinks of the ocean surface wave energy (Tolman 2003). Missed island groups in coarse resolution global models lead to a persistent under-prediction of wave energy blocking. Although the far field errors can be alleviated with sub-grid obstructions, high resolution around islands is still the most appropriate approach for accurate swell prediction close to islands (Chawla and Tolman 2008). One feature of the unstructured SMC grid is that it can also handle multiple resolutions within the same model so that small islands and coastlines are resolved at high resolutions while the vast open oceans are kept at an affordable resolution. This is a very appealing option for operational models as increasing resolution throughout the full model domain to resolve small islands is not economical. The multi-resolution feature of the SMC grid also allows regional models to be merged into one global model, another desirable advance in future operational wave modelling.

This guide covers the implementation of the SMC grid in the WAVEWATCH III (WW3) model (Tolman et al 2002) and description of essential changes required to use the SMC grid. The multi-resolution feature is illustrated with a 3-level global multi-resolution grid and regional applications. Because the ice cover in the Arctic prevents testing of the extension over the whole Arctic, an idealised ocean wave spectral propagation in an ice-free Arctic is used to demonstrate the map-east reference direction method. This spectral propagation program can also be used for testing of the SMC grid input files. Quite a part of this guide is duplication of a published paper (Li 2012) but it would be convenient for users to have all the relevant information in one document. Some references are listed at the end for more details of ocean surface wave theory and development of the WW3 model.

2. Wave propagation on a sphere

The Eulerian ocean surface wave model is based on a 2D spectral energy balance equation. In the 2-D spherical coordinates with longitude λ and latitude φ, the equation is given by

$$
\begin{aligned}
&\frac{\partial \psi}{\partial t}+\frac{\partial F_x}{\partial x}+\frac{\partial\left(F_y \cos\varphi\right)}{\cos\varphi \partial y}+\frac{\partial\left(\dot{k}\psi\right)}{\partial k}+\frac{\partial\left(\dot{\theta}\psi\right)}{\partial \theta}=S \\
&F_x \equiv u\psi - D_x \partial\psi/\partial x \\
&F_y \equiv \upsilon\psi - D_y \partial\psi/\partial y
\end{aligned} \tag{1}
$$

where $\psi(t, \lambda, \varphi, k, \theta)$ is any component of the wave energy spectrum, t is the time, k is the wave number, θ is the spectral direction usually defined from the local east direction, u and υ are the zonal and meridian components of the wave energy propagation speed, D_x and D_y are the diffusion coefficients, and S the source term. The geophysical coordinates x and y are defined locally eastward along the parallel and northward along the meridian, respectively. So their increments are given by $dx = r\cos\varphi d\lambda$, $dy = rd\varphi$, where r is the radius of the sphere. The overhead dot indicates time differentiation along the wave propagation path. The r.h.s S represents all source terms and they are unchanged from the original WW3 model. Note that in WW3 model the wave action $A \equiv \psi/\omega$, where ω is the intrinsic angular frequency of the ocean surface wave, is chosen instead of the wave energy ψ for conservation when ocean current is present. The wave action shares the same equation (1) as the wave energy except that the source term is divided by ω. Hence all propagation schemes for wave energy can be applied on wave action.

The spherical wave energy balance equation (1) differs from its Cartesian counterpart in the meridian differential term by an extra cosine factor, which renders the term undefined (singular) at the Poles. Thus, except for at the Poles, Eq. (1) can be approximated with finite-difference schemes similar to those used in the Cartesian grid. The only difference between the Cartesian and spherical versions of these finite-difference schemes is that the latter has an extra cosine factor. Because the SMC grid retains the lat-lon grid cells, the wave energy balance equation (1) is also valid on the SMC grid.

The diffusion term in (1) may be considered as the sub-grid mixing term because the model wave spectrum represents the spatial average over one grid cell. This diffusion term is usually parameterised to alleviate the so called garden-sprinkler effect (GSE) due to discretization of the wave energy spectrum (Booij and Holthuijsen 1987, Tolman 2002).

One primary physical process that affects surface wave propagation is the depth-induced refraction. Refraction formulations in contemporary surface wave models are based on the linear wave theory, assuming slow-varying ocean depth. The refraction on the SMC grid follows the same formulations in the WW3 (Tolman 1991):

$$\dot{k} = -\xi \mathbf{k}\cdot\nabla h - \mathbf{k}\cdot\nabla U_k \tag{2a}$$

$$\dot{\theta}_{rfr} = -\xi \mathbf{n}\cdot\nabla h - \mathbf{n}\cdot\nabla U_k \tag{2b}$$

where **k** =($k$cosθ, $k$sinθ) is the wave number vector, h is the water depth, ∇ is the 2-D gradient operator, U_k is the ambient current velocity component along the **k** direction, $\xi = \omega/\sinh(2kh)$ will be referred to as the *refraction factor* and and **n** = (-sinθ, cosθ) is a unit vector normal to the **k** direction to the left or at $\theta + \pi/2$. The wave number change rate (2a) is also known as the spectral shift and the direction change rate (2b) is called the refraction rate. More details on derivation of these refraction rates are available in Li (2012).

Wave energy travels along the shortest route on the ocean surface, that is, along great circles on the sphere. So a wave spectral component will not be confined at its defined direction but will shift gradually with latitude along its great circle path, a procedure known as great circle turning (GCT). Assuming the great circle direction is at an angle θ from the local east direction at latitude φ, the product of cosines of these two angles is conserved on the great circle path, that is, $\cos\theta\cos\varphi = const.$, which provides a simple rule for navigation along great circles and leads to the following GCT rate along the propagation direction

$$\dot{\theta}_{gct} = -\left(c_g / r\right)\cos\theta\tan\varphi \tag{3}$$

where c_g is the wave group speed defined by

$$c_g = c_{gd}\left(\tanh(kh) + kh/\cosh^2(kh)\right) \tag{4}$$

in which $c_{gd} = g/2\omega$ is the group speed in deep waters. The net wave direction changing rate used in (1) for the SMC grid is then the sum of the refraction rate (2b) and the GCT rate (3).

3. Numerical schemes on a SMC grid

Scalar advection schemes on the SMC grid are described in Li (2011). Here summarised are other terms in (1) and treatment of advection and diffusion on the multi-resolution SMC grid. It also tackles the polar problem with vector components at high latitudes.

3.1. SMC grid cell and face arrays

A global SMC grid is shown in Fig.1. For clarity, only the Arctic region is shown here. The highest resolution of the SMC grid (for size-1) cell is set to be $\Delta\lambda$ = 360º/(1024*4) = 0.3515625º/4 and $\Delta\varphi$ = 180º/(768*4) = 0.234375º/4 and the latitudinal grid length is about 6 km. The SMC grid uses only the sea points or cells and refines the resolution by two levels to 6 km around islands and coastlines, resulting in a global 3-level (6-12-25 km) SMC grid on ocean surface. This SMC grid will be referred to as the SMC6-25 grid. Cells are merged longitudinally at high latitudes following the same rules in Li (2011) to relax the CFL restriction. A unique 5-element integer array is assigned to each cell to hold its SW corner *x*-, *y*-indices (*i, j*), cell *x*-, *y*-sizes (Δi, Δj), and water depth (*h*), as illustrated in Fig.2. The *x*- and y-indices are measured in size-1 cell increment so the cell centre latitude and longitude can be worked out with

$$\varphi_j = \left(j_0 + j + 0.5 * \Delta j\right)\Delta\varphi; \qquad \lambda_i = \left(i_0 + i + 0.5 * \Delta i\right)\Delta\lambda \tag{5}$$

where i_0 and j_0 are the origin of the cell *x*- and *y*-indices relative to the zero-meridian and the Equator, respectively. For the SMC6-25 grid, the origin of the grid indices is set at zero-meridian on the Equator so both i_0 and j_0 are zero. The mapping rule (5) is exactly the same as that for the lat-lon grid cells except for that the SMC grid cells are not arranged in spatial sequence (hence is called an unstructured grid) and their sizes may change by a multiple of 2 (size-1, size-2, size-4, …). The depth *h* is also rounded to an integer so the whole cell array can be declared as an integer array. The cells are listed as a 1-D array and sorted by their *y*-size for use of sub-time steps on refined cells. Please note that the sorting is on the *y*-size not the *x*-size because the cell *x*-size may change on the same resolution level due to the longitudinal merging at high latitudes. The cell *y*-size will be in ascending order in the sorted cell array list and the number of cells for each resolution level (of a given *y*-size) is listed on the first line of the cell array file after the total cell number. This cell number counts will be used for declaring the cell array variable and setting the sub-loops for the propagation.

It should be emphasized that the cell size has to be increased no more than 1 level for any neighbouring cells, that is, around a size-1 cell the neighbouring cells can be either size-1 or size-2. Similarly, size-2 cells can be linked to cells of the same size-2 or either 1-level down (size-1) or 1-level up (size-4). This 1-level size change rule ensures resolution varies gradually and simplifies the face flux formulation. Putting cells of more than 1 level difference in sizes sided by side would jeopardise the present face array generating program.

Once the cell arrays are compiled in the sorted order, cell face arrays can be generated with an extra FORTRAN code. Cell faces are named by its normal velocity components as *u*- or *υ*-faces. A 7-element integer array is pre-calculated for each face to store its face position, size, and its upstream-central-downstream (UCD) cell indices. An extra *y*-size integer is added for the υ-face array for sorting purposes. Face sizes are chosen to be the minimum size between the two neighbouring cells. For a cell face neighbouring two cells of 1-level below, the face is divided into two faces of the lowered level size. This minimised face size ensures one face links two cells only. The face arrays are also sorted by its *y*-size so that the multi-resolution advection/diffusion loops can be divided into multi-step sub-loops. The total face number and sub-level face numbers are listed on the first line of the face array file for propagation and mapping purposes. The face arrays are used to calculate the advection-diffusion and the depth gradient.

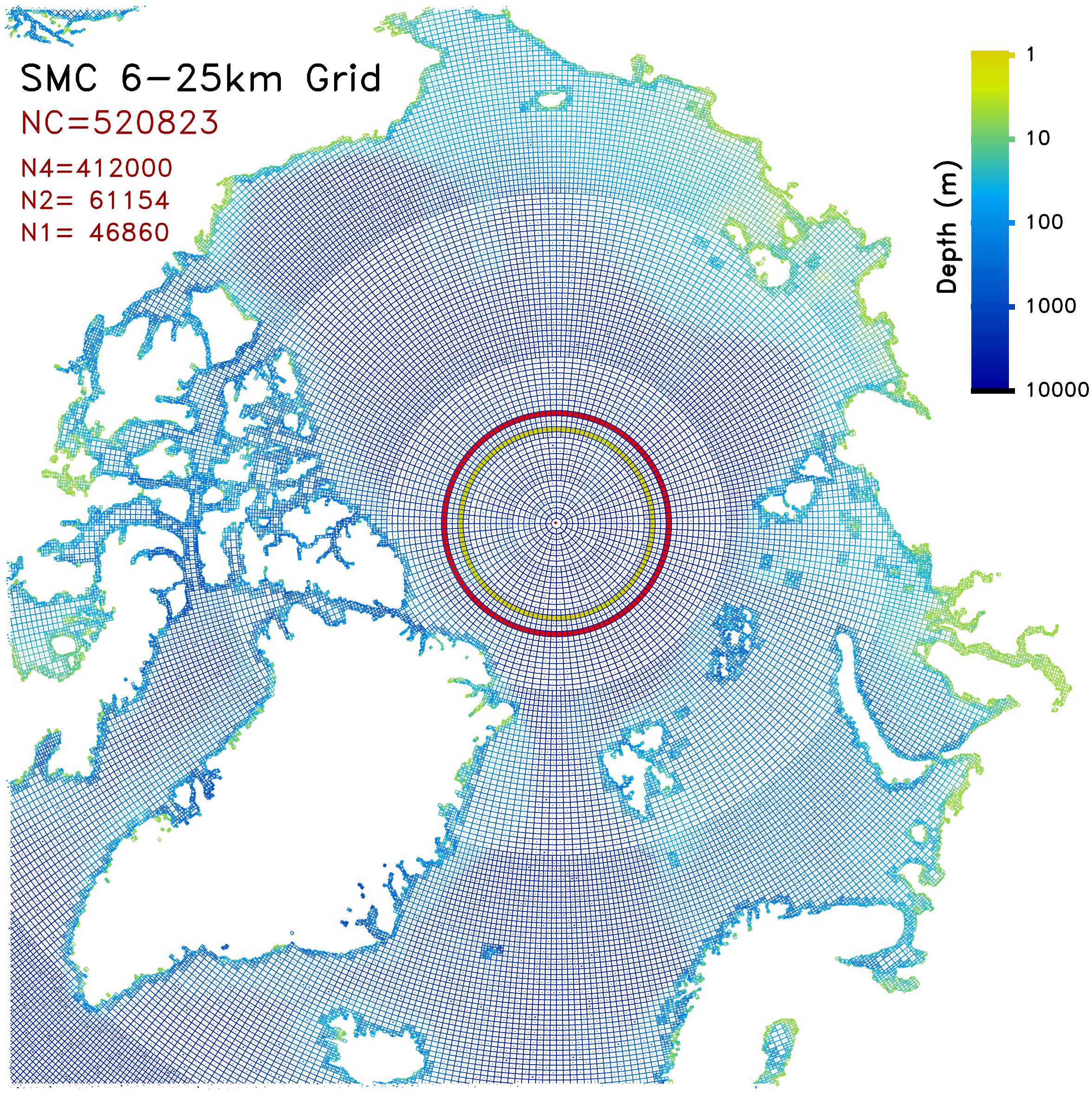

Fig.1. The Arctic part of the SMC6-25 grid.

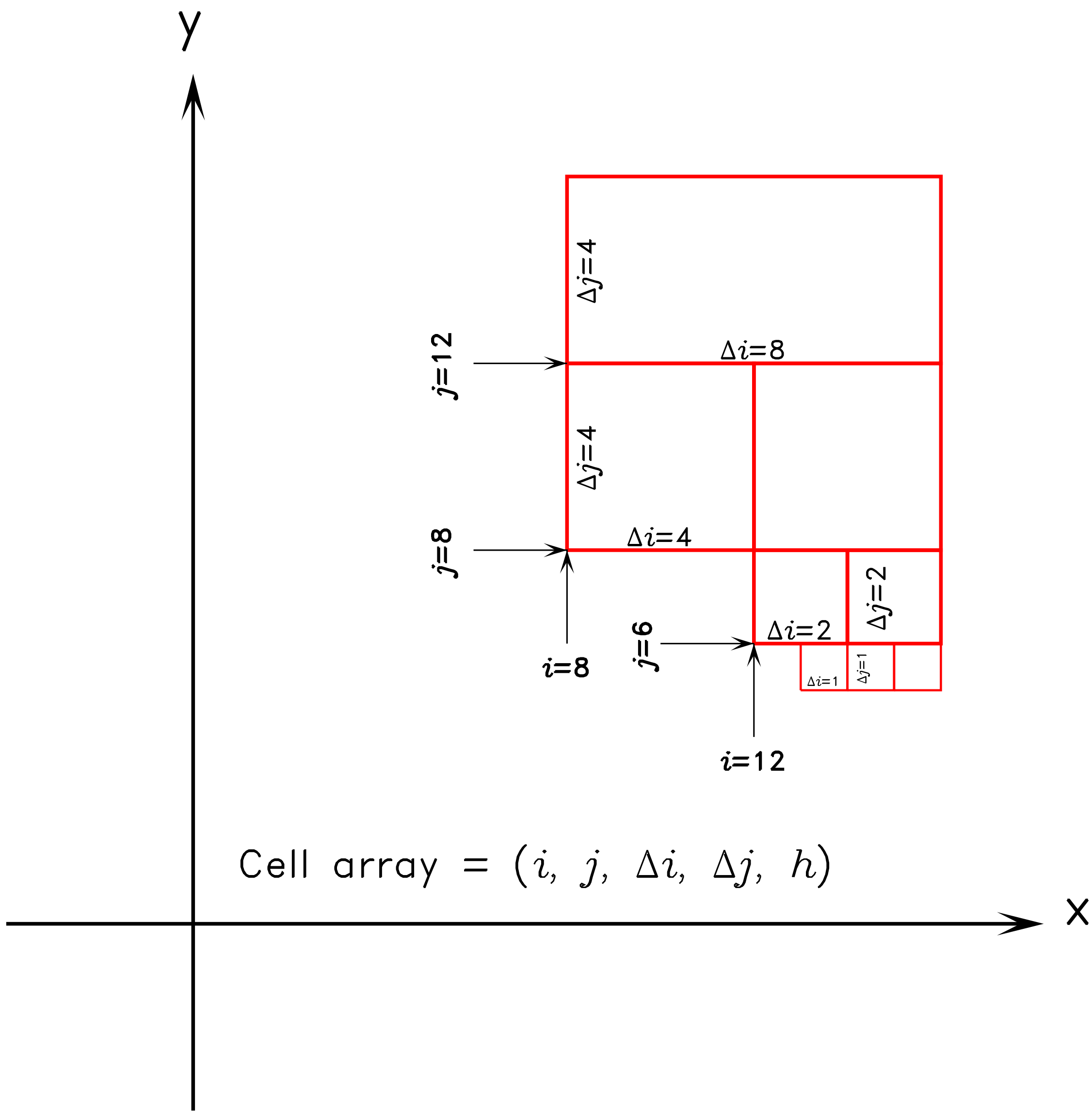

Fig.2. Illustration of SMC grid cell arrays.

3.2. Advection-diffusion schemes

The l.h.s terms in (1) are calculated with time-splitting approaches by combining the first (time differential) term with each of the other 4 terms. The advection-diffusion terms are discretised on the SMC grid with one flux loop and one cell loop for each dimension. Note that the diffusion term used here is slightly different from the original GSE smoothing term (Booij and Holthuijsen 1987). The original diffusion term is designed to enhance the transverse smoothing because a first order upstream advection scheme is used and it has already introduced strong smoothing along the wave propagation direction. The asymmetrical diffusion results in a cross term in Cartesian coordinates. In this SMC grid wave model, the advection is estimated with an upstream non-oscillatory 2nd order (UNO2) scheme (Li 2008), which is adapted from the MINMOD scheme (Roe 1985). As the implicit diffusion of the 2nd order advection scheme is much smaller than that of the first order scheme, the diffusion term is simplified to be isotropic so the cross-term vanishes. Besides, the refraction and GCT term provides extra directional smoothing, which makes the total smoothing biased towards the transverse direction, similar to the original asymmetrical smoothing term.

The advection flux with the UNO2 scheme and the diffusion flux with a central-space finite difference scheme for a u-face between the central and downstream cells are merged into a single flux, given by

$$\Delta F_x = \left(u\,\psi * - D_x G_{DC}\right) l_u \Delta t \tag{6}$$

where ψ^* is the mid-flux value evaluated with the UNO2 scheme (see Eq. (6) in Li 2008), $G_{DC} = (\psi_D - \psi_C)/(x_D - x_C)$ is the gradient between the central and downstream cells, l_u is the u-face length and Δt is the sub-time step. Both the advection and diffusion schemes are of 2nd order accuracy. The diffusion coefficient, $D_x = D_y$, is specified by the spectral component propagation speed, directional bin width and a user input swell age parameter as the transverse diffusion coefficient D_{nn} in the original model. In the presence of an ambient ocean current, the wave energy propagation speed in the x-direction should be the sum of the group speed and current speed components, that is, $u = c_g \cos\theta + U_x$.

A temporary net-flux variable, F_{net}, is used for each cell to gather all fluxes into the cell before it is used for the cell value update. The flux (6) is added to the downstream cell net-flux variable and subtracted from the central cell net-flux variable at the same time for energy conservation. The use of face sizes and the net flux variables allow fluxes from different sized faces to be added up in proportion to their face sizes. After the face loop is completed, each cell value is updated in a cell loop by

$$\psi^{n+1} = \psi^n + F_{net} / \left(l_x l_y\right) \tag{7}$$

where $l_{x/y}$ is the cell x/y-length. The cell y-length is required for x-flux update to cancel the face length used in sum of the fluxes in proportion to the u-face length. The υ-face fluxes are calculated similarly except for the additional latitude cosine factor.

For the multi-resolution SMC6-25 grid, the face and cell loops are sorted into 3 sub-loops according to their y-sizes, thanks to the unstructured nature of the SMC grid. Advection-diffusion terms for the refined 6- and 12-km cells are calculated at ¼ and ½ of the base level time step, that is, the 6-km flux and cell loops are done twice before the 12-km flux and cell loops are calculated once. The base level flux and cell loops are only calculated at each base level time step. The temporary net-flux variable is used to accumulate fluxes between different levels and is reset to zero once it is used for its cell update. The simple loop–regrouping technique for multi-resolution SMC grid allows a smooth transfer from a single resolution SMC grid to a multi-resolution grid with optimised efficiency.

Another feature of the SMC grid is the unification of boundary conditions with internal flux evaluations. Cell faces at coastlines are assumed to be bounded by two consecutive empty cells when the face arrays are generated. Thus, any wave energy transported into these empty cells will disappear, and no wave energy will be injected out of these zero cells into any sea cells. This convenient setup conforms to the zero wave energy boundary condition at land points used by ocean surface wave models and allows all the boundary cell faces to be treated in the same way as internal faces in one face loop. In addition, the periodic boundary condition for a global model is automatically included by the unstructured grid. So short boundary loops are avoided in the SMC grid propagation schemes and the full face and cell loops are streamlined for vectorization and parallelization.

An additional benefit of using two consecutive zero-boundary cells beyond the coastline is the complete blocking of wave energy by single-point islands. On a conventional lat-lon grid, wave energy can 'leak' through a single-point island due to the interpolation with neighbouring sea points in transport schemes which use a 5-point stencil like the UNO2 scheme. In the SMC grid, any single-point island is extended with two zero cells beyond its boundary face. As a result, wave energy cannot pass through such 'expanded island'.

Nevertheless, sub-grid obstruction scheme from the original WAVEWATCH III model is kept to count for islands unresolved by the 6-km resolution. The sub-grid obstruction scheme follows the approach of Hardy et al (2000) with some modifications (Tolman 2003).

For the updated version 5 WW3 model, an optional 3rd order advection UNO3 scheme (see Li 2008) is added so users may replace the default UNO2 scheme with the UNO3 scheme by defining a namelist (PSMC) variable UNO3 = .TRUE. in the ww3_grid.inp file. As UNO3 scheme is less diffusive than the UNO2 scheme, an additional 1-2-1 weighted smoothing term is also available by defining the PSMC namelist variable AVERG = .TRUE. in the ww3_grid.inp file. The default diffusion term is still in effect for the UNO3 scheme and users may adjust this term with the swell age parameter as in the default UNO2 scheme case.

3.3. Refraction and spectral shift schemes

It should be emphasized that the linear surface wave theory is only valid when the water depth is non-zero (Falnes 2002). When h approaches zero, for instance, the refraction rate (2b) becomes undefined because the ξ factor approaches infinity ($\xi \sim 0.5\sqrt{g/h}$). It is then customary in wave models to use a minimum water depth for the refraction term. A minimum water depth of 10 m is recommended and the refraction factor will then be less than 0.5.

Apart from shallow water depth, steep ocean floor and large time step may also result in a large refraction rate. For instance, if the discrete depth gradient is assumed to be $\Delta h/\Delta x$ = 0.1 and time step is Δt = 1000 s, the maximum refraction angle per time step might be $\Delta t \Delta h / 2\Delta x \sim 50$ rad or about 8 full circles, which is no longer physically meaningful and is too large to fit into any advection-like refraction schemes used in contemporary wave models. One way to avoid this unrealistic large refraction increment is to use a small time step but this usually turns out to be too restrictive for wave models. Since refraction in a wave model is usually a minor process and is confined to coastal regions, the refraction increment is simply reduced to fit for the advection-like CFL condition in some wave models (WAMDI group 1988, Booij et al 1999, Tolman etal 2002). The CFL condition requires the refraction angle increment per time step to be less than one directional bin width (about 10º) and, of course, reduces the refraction effect. The latest version of the WAVEWATCH III model uses sub-time step to relax this restriction on the refraction term.

Here for the SMC grid wave model, a rotation scheme is substituted for the advection-like scheme to estimate the refraction term so that the CFL limit can be avoided. The rotation scheme is similar to a re-mapping advection scheme and is unconditionally stable. Although the rotation scheme does not have any limit on the refraction increment, the refraction angle should not pass beyond the depth gradient line (where $\mathbf{n} \cdot \nabla h = 0$) as stated in the refraction rate (2b). This physical limiter on the total refraction angle is included in the rotation scheme. The angle between the spectral direction and the depth decrease direction is calculated by:

$$\gamma = \cos^{-1}\left[-\left(h_x \cos\theta + h_y \sin\theta\right) \Big/ \sqrt{h_x^2 + h_y^2}\,\right] \qquad (8)$$

where h_x and h_y are the water depth gradient along x and y axis, respectively. Because FORTRAN function ACOS returns value between 0 and π, the maximum refraction angle (absolute value) is then chosen to be less than $\pi/2$ with $\Delta\theta_{mxrfr} = \min(\eta, \gamma, \pi - \gamma)$. The constant η ($< \pi/2$) is a user-defined maximum refraction angle to reduce the refraction effect if required. If η is set to be less than one directional bin width, the rotation scheme will be equivalent to the original advection-like scheme in the WAVEWATCH III model without using sub time steps. For the present comparison study, the refraction limiter is set to be $\pi/3$. This refraction limiter may prevent all directional components from converging at the depth gradient direction within one time step, which may result in unrealistic large wave energy like caustics in ray tracing models. It also creates room for merging the refraction with other directional changing terms, such as the refraction by ambient current and the GCT term.

The GCT term (3) can be fit into an advection-like scheme because it is usually less than one directional bin (~ 10º). For instance, if the time step is less than 900 s, the GCT angle (3) will be less than 1º per time step below 85º latitude, as the wave propagation angular speed, c_g/r, is on the order of 10^{-6} rad s^{-1}. However, as the refraction term is calculated with a rotation scheme in the SMC grid model, the GCT term is simply appended to the refraction term to form a total rotation angle. The rotation subroutine rotates each directional component by the combined angle and partitions its energy into the two directional bins which the rotated one strides across after the rotation. This simple rotation subroutine not only removes the time step restriction on the refraction angle but also adds an implicit diffusion in the θ direction because its implicit diffusivity is equivalent to that of the first order upstream scheme. This additional smoothing in the transverse direction is desirable for wave models to mitigate the GSE.

The spectral shift term, fourth in (1), is calculated with an advection-like UNO2 scheme in the k-space because the spectral shift is usually small enough to meet the CFL condition. The term is calculated at the base time step for all cell spectra.

3.4. The polar problem

The ocean surface wave energy spectrum is usually defined as discrete directional components from a reference direction at the local east and each directional component is assumed to be a scalar in wave propagation. This scalar assumption has been taken for granted in finite difference schemes, such as, calculation of the local gradient, $G_{DC} = (\psi_D - \psi_C)/(x_D - x_C)$, where the vector components ψ_D and ψ_C for the two neighbouring cells are assumed to be at the same direction, that is, to be treated as a scalar. This scalar assumption is a good approximation for a global wave model when the ice covered Arctic area is excluded. However, the scalar assumption becomes erroneous at high latitudes on a reduced grid since the change of direction over one grid-length grows too large to be ignored. For instance, in the SMC6-25 grid (see Fig.1) there are 8 cells immediately around the polar cell, the local east direction changes by 45º over one cell length. The invalid scalar assumption based on local east reference direction in the polar region prevents extension of ocean surface wave models at high latitudes. This problem can be avoided by switching to a fixed reference direction, for instance, the map-east direction as viewed on a stereographic projection of the polar region. Assuming the angle from the map-east to the local east is α, the wave spectral component for a given direction of angle θ from the local east will have an angle $\theta' = \theta + \alpha$ from the map-east. Its zonal and meridian group speed components are then given by

$$\begin{aligned} c_g \cos\theta &= c_g \cos(\theta' - \alpha) \\ c_g \sin\theta &= c_g \sin(\theta' - \alpha) \end{aligned} \tag{9}$$

Note that the polar cell does not have a local east direction so the velocity could not be defined at the Pole as zonal and meridian components. In the SMC grid, however, only the meridian velocity component at the edge of the polar cell is required and there is no need to define the velocity at the polar cell centre. This is one of the advantages of using a polar cell centred at the Pole. Nevertheless, velocity components at the Pole can be defined in the fixed reference system but they could not be converted into the local east system.

Because a given direction θ' from the map-east is constant in the Arctic region, the spectral component in the map-east system can be treated as a scalar for transport in the polar region. For the velocity in a dynamical model, its components along the map-east ($\theta' = 0$) and map-north ($\theta' = \pi/2$) can also be approximated as a scalar in the polar region. Their transport velocity components in the standard grid are then given by (9) after substituting their corresponding component values (*u'* and *v'*) for c_g, respectively. The polar cell can hold velocity or wave spectrum in the map-east system as scalars for transport but they do not need to be converted into the local east system.

This map-east direction can be conveniently approximated with a rotated grid with its rotated pole on the Equator. The standard polar region becomes part of the 'tropic region' in the rotated grid so the longitudinal direction of the rotated grid can be substituted for the map-east direction. For instance, if the rotated pole is at 180ºE on the Equator, the angle α from this map-east to the local east at longitude λ and latitude φ within the Arctic region can be worked out with:

$$\alpha = \mathrm{sgn}(\cos\varphi \sin\lambda)\arccos\left[\frac{\cos\lambda \sin\varphi}{\sqrt{1-(\cos\lambda\cos\varphi)^2}}\right] \tag{10}$$

If the map-east is used within the Arctic region and local east in the rest for definition of the wave spectrum, there will be no fixed corresponding components between the two systems because α varies with longitude and latitude. For this reason, wave spectra defined by local east could not be mixed up with those defined from the map-east and the Arctic region using the map-east reference direction has to be separated from the rest which uses local east reference directions. In the SMC grid shown in Fig.1, the reference direction change is set between the 3rd (at about 83º) and 4th (at 86.4º) size-changing parallels (see definition in Li 2011), where the local east direction changes less than 3º over one cell length as there are 128 cells in one row. The Arctic part and the rest (will be referred to as the *global part*) are linked together through 4 over-lapping rows. Wave spectra in the lower two of the 4 over-lapping rows in the Arctic part are updated with wave spectra from the global part after they are rotated anticlockwise by α. Wave spectra in the upper two rows of the 4 over-lapping rows in the global part are updated with wave spectra from the Arctic part after a clockwise rotation by α. Because of the unstructured nature of the SMC grid, the Arctic cells are appended behind the global part in the single cell list for propagation. The two parts can be conveniently separated by using sub-loops. The overlapping rows are treated in the same way as other cells so the propagation is calculated together for both parts. Wind direction and other direction related source terms have to be modified within the Arctic part to use the map-east reference direction.

If only the velocity components are dealt with within the Arctic (such as in a dynamic model), there is no need to work out the angle itself. The cosine and sine of the rotation angle will be enough for velocity conversion between the map-east and local east system. The rotation angle cosine and sine are given by

$$\cos\alpha = \frac{\cos\lambda\sin\varphi}{\sqrt{1-(\cos\lambda\cos\varphi)^2}}, \qquad \sin\alpha = \frac{\sin\lambda}{\sqrt{1-(\cos\lambda\cos\varphi)^2}}, \tag{11}$$

The conversion between the map-east velocity components *u'* and *v'* and the local east velocity components *u* and *v* are given by

$$\begin{pmatrix} u' \\ v' \end{pmatrix} = \begin{pmatrix} \cos\alpha & -\sin\alpha \\ \sin\alpha & \cos\alpha \end{pmatrix}\begin{pmatrix} u \\ v \end{pmatrix}, \qquad \begin{pmatrix} u \\ v \end{pmatrix} = \begin{pmatrix} \cos\alpha & \sin\alpha \\ -\sin\alpha & \cos\alpha \end{pmatrix}\begin{pmatrix} u' \\ v' \end{pmatrix} \tag{12}$$

That is, the local east velocity vector is rotated anticlockwise by the angle α as viewed in the map-east system. The wind component relationship (12) may also be used in the Arctic part to convert the local east wind to the map-east wind for wave model source terms.

The great circle turning (GCT) term (see Eq. 3) has to be modified in the Arctic part to use the rotated grid latitude, which is close to zero in the Arctic part because the rotated Equator passes the North Pole. If the Arctic part is kept small around the polar region (like above 85ºN in the SMC625 grid), this GCT term becomes negligible. The refraction term (see Eq. 2) retains the formulation in the Arctic part except for that the gradients of water depth and current component along the wave direction have to be rotated to the map-east system. As the Arctic Ocean above 85ºN is considered deep for wind waves, the refraction is also negligible in the small Arctic part.

3.5. Spatial field gradient on a SMC grid
The spatial gradient of a given field variable on a SMC grid or at a sea point may be required for other terms, such as wave scattering or bottom friction. The SMC grid module contains a convenient subroutine, `SMCGradn(HCel, GrHx, GrHy)`, which calculates the spatial gradients, `GrHx(1:NSEA)`, `GrHy(1:NSEA)`, of the given field `HCel(-9:NSEA)`. Note that the input field is extended from the normal range (`1:NSEA`) to (`-9:NSEA`) for the SMC grid. The `HCel(-9:0)` should be assigned the boundary values (on land points) used for this given field. For water depth as an example, set `HCel(-9:0)=0`. See the subroutine `SMCDHXY` in `ftn/w3psmcmd.ftn` for a calling example of this gradient subroutine.

4. Input files for SMC option

The regular lat/lon grid WW3 wave model requires input files for wind forcing, sea-ice coverage, water depth, sub-grid obstruction and land-sea masking. For the SMC grid option these regular grid input files are no longer required and they are replaced with sea-point only files. The water depth is stored in the last column of the cell array file in unit of meter. If the accuracy at a meter is not enough, users may use other unit (such as cm) and convert the depth integer back to unit of meter inside the ww3_grid program. Using integer to represent water depth in the cell array is to ensure the cell array is completely an integer array. For this reason a corresponding regular grid at the base level resolution of the SMC grid is used to set up the WW3 model for the SMC grid option. For example, a 25km regular lat-lon global grid is used for setting up the input files for the SMC6-25 grid. When compiling the WW3 executables, the spherical regular lat/lon grid option should be selected and the propagation options (PR3 UQ as default) should be replaced by the SMC option. Most of the WW3 model will work the same way as on the regular grid except for the propagation (advection, diffusion, refraction, and GCT) part, which will be calculated with the newly added SMC module. Extra input files for the SMC module are required for the ww3_grid program to generate the mod_def.ww3 file. These extra input files include the SMC grid cell and face arrays and the modified ww3_grid.inp file. If input boundary condition is required for a regional model on a SMC grid, an extra boundary cell file is also required for the ww3_grid program. If the Arctic part is included, they require extra cell and face array files for the Arctic part as well. These Arctic part cell and face arrays will be merged with the global part cell and face arrays inside the ww3_grid program.

Modifications in the ww3_grid.inp file include:
i) Adding a new namelist for SMC grid propagation module
```
  &PSMC DTIME=39600.0, LATMIN=85.0, RFMAXD=36.0,
        LvSMC=3, JEQT=1344  /
```
where DTIME is the swell age (in unit of s) used to define the smoothing (diffusion) coefficient, LATMIN is the minimum grid length latitude and FRMAXD is the maximum refraction angle in degree. The swell age has the same meaning as in the regular grid WW3

model and it has to be adjusted according to the base-level grid length and the advection time step (diffusion is calculated at the same time step as advection) to ensure the maximum Fourier number is less than 1 or usually set to be 0.5. A guide rule for the maximum swell age T_s is given by

$$T_s \leq \frac{6}{\Delta t_a}\left(\frac{\Delta x_0}{c_{gm}\Delta\theta}\right)^2 \tag{13}$$

in which Δt_a is the advection time step, Δx_0 is the base level grid length on the Equator, $\Delta\theta$ is the directional bin width (in radian) and c_{gm} is the maximum group speed in the model spectral range (usually at the lowest frequency end). If the swell age is set too large, the diffusion term will become unstable and eventually bring the model to a crash. It would be convenient if the swell age was reduced automatically inside the model when users accidentally set it too large. This automatic adjustment, however, has not been set up yet.

The minimum grid length latitude parameter is for the regular grid of the WW3 model. It is used for control of the regular grid diffusion and GCT terms. As these restrictions have been relaxed in the SMC grid, this parameter is simply set to be the highest latitude of the model domain. The maximum refraction angle is the limiter for the refraction rotation scheme. It is recommended to be less than 60 degree to avoid caustic-like focus of spectral energy. Setting it equal to one directional bin width will bring the refraction rotation scheme to be equivalent to the regular grid refraction term.

The LvSMC integer represents the number of levels of the multi-resolution SMC grid. The above quoted line is for the SMC6-25 grid, which has 3 levels: the 6km, 12km and the base level 25km. The JEQT integer (1344) is a shifting number for conversion of the SMC grid cell *y*-indices to the regular grid *j* indices. It is equal to the distance from the regular grid *y*-origin to the SMC y-index origin and divided by the SMC size-1 unit length. Because the regular 25km grid y-indices starts from southern boundary of the model domain while the SMC6-25 cell y-indices are referred from the Equator, the SMC6-25 cell *j* indices have to be shifted by this number for mapping with the regular grid *y*-indices. There is a similar namelist integer parameter ISHFT for the x-index conversion to the regular grid *i*-indices. As the SMC6-25 cell *x*-indices share the same origin as the regular grid (at zero meridian) this number simply takes the default value 0. Also note that, the SMC6-25 cell indices are measured from the smallest cell (size-1) while the 25km regular grid is at the base level (size-4). So SMC6-25 cell indices are 4 times larger than the regular grid ones.

If the model needs boundary conditions, users should set another PSMC namelist integer NBISMC, which is the number of boundary cells. A non-zero number will invoke extra lines to read the boundary cell list from a file and setup boundary condition interpolation arrays for the model. If not defined, it will take the default value 0 and tell the ww3_grid to skip those lines as there is no boundary conditions are required. Note that smc grid boundary conditions are set up by the boundary cell list (the sequential number of the boundary cells in the full cell array list) instead of using the masks. To generate boundary conditions for other models, however, the smc grid uses the normal longitude and latitude settings as a regular lat-lon grid model. This is also true for generating boundary conditions for the smc grid model. Users need to convert the cell list into corresponding list of lat-lon pairs. The lat-lon pair list does not need to be in the same order as the boundary cell list.

If users like to use the 3rd order UNO3 scheme and the additional averaging term, the two logical parameters UNO3 and AVERG could be added to the PSMC namelist:

```
 &PSMC DTIME =39600.0, LATMIN=85.0, RFMAXD=36.0,
       UNO3=.TRUE., AVERG=.TRUE., LvSMC=3, JEQT=1344  /
```

ii) Add lines to read the SMC cell and face array files after reading the regular grid depth file (which line is still kept to read the minimum depth parameter though the regular grid depth file is not actually read for SMC grid):

```
32  1  1  '(....)'  'S6125MCels.dat'
33  1  1  '(....)'  'S6125ISide.dat'
34  1  1  '(....)'  'S6125JSide.dat'
31  1  1  '(....)'  'S6125Obstr.dat'
```

These lines are similar to those for reading the regular grid water depth. The regular grid sub-grid obstruction file read line is moved after the cell and face array files because the smc cell only obstruction file requires the cell array for mapping the obstruction ratio.

iii) Additional lines for Arctic cell and face arrays if the Arctic part is included:

```
$   Boundary cell id number list file is required if NBISMC is non-zero.
$   The cell id number should be the sequential number in S625MCels.dat.
$   Boundary cell spectral input data should be produced from a regular
$   lat-lon grid model for the listed boundary cells.  JGLi18Dec2012
$ 35  1  1  '(....)'  'S6125Bundy.dat'
$
$   Extra cell and face arrays for Arctic part.  JGLi16Jan2014
  36  1  1  '(....)'  'SMC625BArc.dat'
  37  1  1  '(....)'  'S625AISide.dat'
  38  1  1  '(....)'  'S625AJSide.dat'
```

Note the boundary cell line is commented off as no boundary condition is required for the SMC6-25 model. The regular grid masks file input line is kept though the masks file is not read actually for SMC6-25 grid.

```
  39  1  1  '(....)'  'NAME'  'S625Masks.dat'
```

Once these input files are put in place, the mod_def.ww3 is generated with the ww3_grid program as for the regular grid model. The SMC grid WW3 model can then be run the same way as a regular grid model. See the WW3 manual for running the ww3_grid and the ww3_shell program.

Output from the SMC grid WW3 model can be saved as the regular base-level lat-lon grid ones or in the raw ww3 format output. The former regular grid output will lose the refined resolutions. The raw ww3 format saves output at all sea points, i.e., all the SMC cells, and requires re-mapping with the cell array for visualisation. A visualisation post-processing program for the SMC grid ww3 format output is still in its development stage.

5. Spectral propagation test

There is a pure spectral propagation test for the SMC grid input files before they are used for the WW3 wave model. This spectral test can also be used for validation of other propagation features, such as the proposed map-east direction method in the Arctic and the rotation scheme for the wave refraction. An idealised wave propagation test on the SMC6-25 grid in an ice-free Arctic is used here for demonstration. The test includes all the 4 terms (advection, diffusion, refraction and GCT) in (1) but does not have any source term. The transient zone from the global to the Arctic parts is around 86ºN and the map-east reference direction is used within the Arctic part (area within the red ring in Fig.2).

A constant wave spectrum is assigned to all cells within a 3.75º radius from the N Pole. The wave spectrum has 36 directions and a fixed frequency at 0.0625 Hz or period T = 16 s.

Because all frequencies show the same directional pattern, one frequency is sufficient for this demonstration. The initial wave spectrum is defined by

$$E(\theta) = \begin{cases} E_0 \cos^2(\theta - \theta_p), & for \left|\theta - \theta_p\right| < \pi/2 \\ 0, & Otherwise \end{cases} \tag{14}$$

where $E_0 = 50/\pi$ is a constant, θ_p is the peak direction. The transported spectrum is integrated as the wave height, $H = \sqrt{\int E d\theta}$, similar to the SWH used in wave models apart from a constant factor. The gravity depth is about 64 m for the given frequency (0.0625 Hz) ocean surface wave and its group speed is about 12.5 m s^{-1} in deep waters. The time step is 300 s for the smallest (6 km) cells and is increased to 600 and 1200 s for the 12 km and 25 km cells, respectively, resulting in a maximum Courant number of 0.929.

The initial wave height field is shown in the row (a) of Fig.3 and its non-zero wave height is constant 5 units. Note the wind-sea spectrum (18) has a peak direction θ_p from its reference direction. The peak direction is set to be 45° towards the northeast for the two round patches and the southern belt as indicated by the spectral roses in Fig.3. For the northern belt the peak direction is at -45° towards the southeast. To assess the map-east method, another round patch of the same size as the Arctic one is initialised in the Atlantic close to the Equator (centred at 33°W 5°N). As long as the two patches share similar propagation pattern, the map-east method may be considered to be equivalent to the local east method. Because the Arctic and global parts use different reference directions, the peak direction of the initial spectrum varies with longitude in the global part. Inside the Arctic part, however, the reference direction is fixed at the map-east so the initial spectral peak direction is constant for all non-zero cells there. This is why the initial Atlantic round patch is placed near the Equator where the direction has the minimum change rate with longitude.

The middle row (b) of Fig.3 shows the idealised wave propagation result after 40 hrs. The initial waves have travelled about 1800 km and typical wave propagation features are revealed. The Arctic patch is almost out of the Arctic part and shows a similar distribution as the Atlantic patch. The northern belt in the Atlantic has passed the British Isles and reached the Canary Islands. The blocking effects of the Azores islands are clearly illustrated. The northern belt in the Pacific shows the cutting effect by the Aleutian Islands. The southern belt has reached the southern coast of Australia and revealed the blocking by New Zealand and other Pacific islands. The stretching effect around the gravity depth is visible in the Great Australia Bight where the wave height (in colour green) is lower than those on the deep side (yellow-orange) and near the coastlines (orange-red). This stretching effect is difficult to see in wave models because it is usually muffled up by wind sea and other propagation effects, such as dispersion and refraction.

The lower row (c) of Fig.3 shows the propagation results after 80 hrs. By then the northern belt has cut through the Hawaii Islands, revealing their detailed blocking effects by the 8 main islands. The G25 and SMC25 grids can only resolve 4 islands out of the Hawaii archipelago. The southern belt is now abreast with the northern coast of Australia, pulling through the oceanic islands. The highest 6 km resolution in this SMC6-25 grid is, however, still not enough to show the atolls or coral reefs in the French Polynesian islands as demonstrated by Chawla and Tolman (2008) in a high resolution regional model and sub-grid obstruction is required to represent the fine structure. Also note in row (c) of Fig.3, the slow GCT and GSE smoothing effects manifest themselves with the smoothly spreading of wave energy in the Southern Ocean and quickly filling up the shadows behind the wave-blocking islands. Smoothed wave propagation indicates that the input files for the SMC grid are set properly and are ready to be used for the wave model.

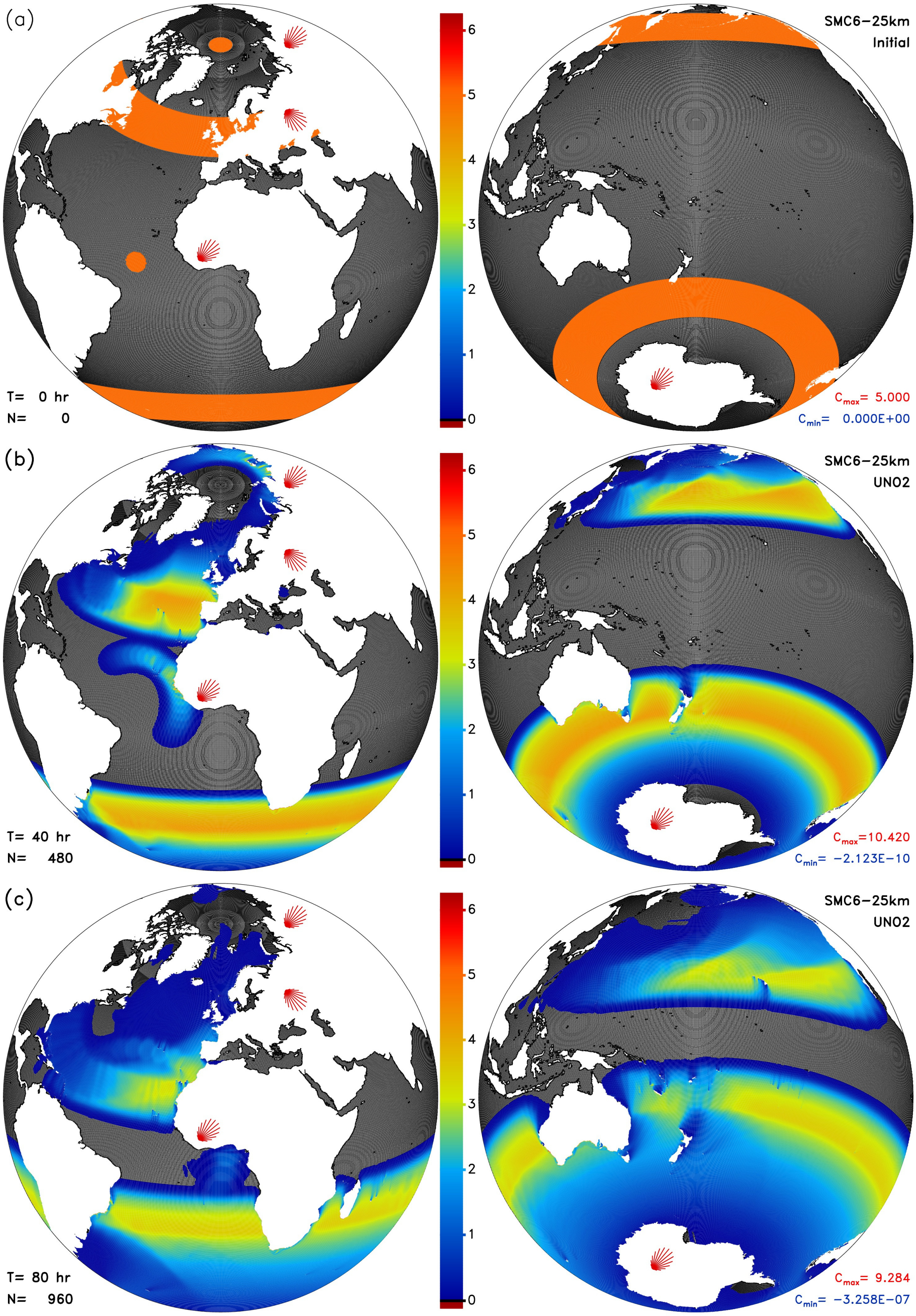

Fig.3. Idealised spectral wave energy propagation on a global SMC6-25 km grid.

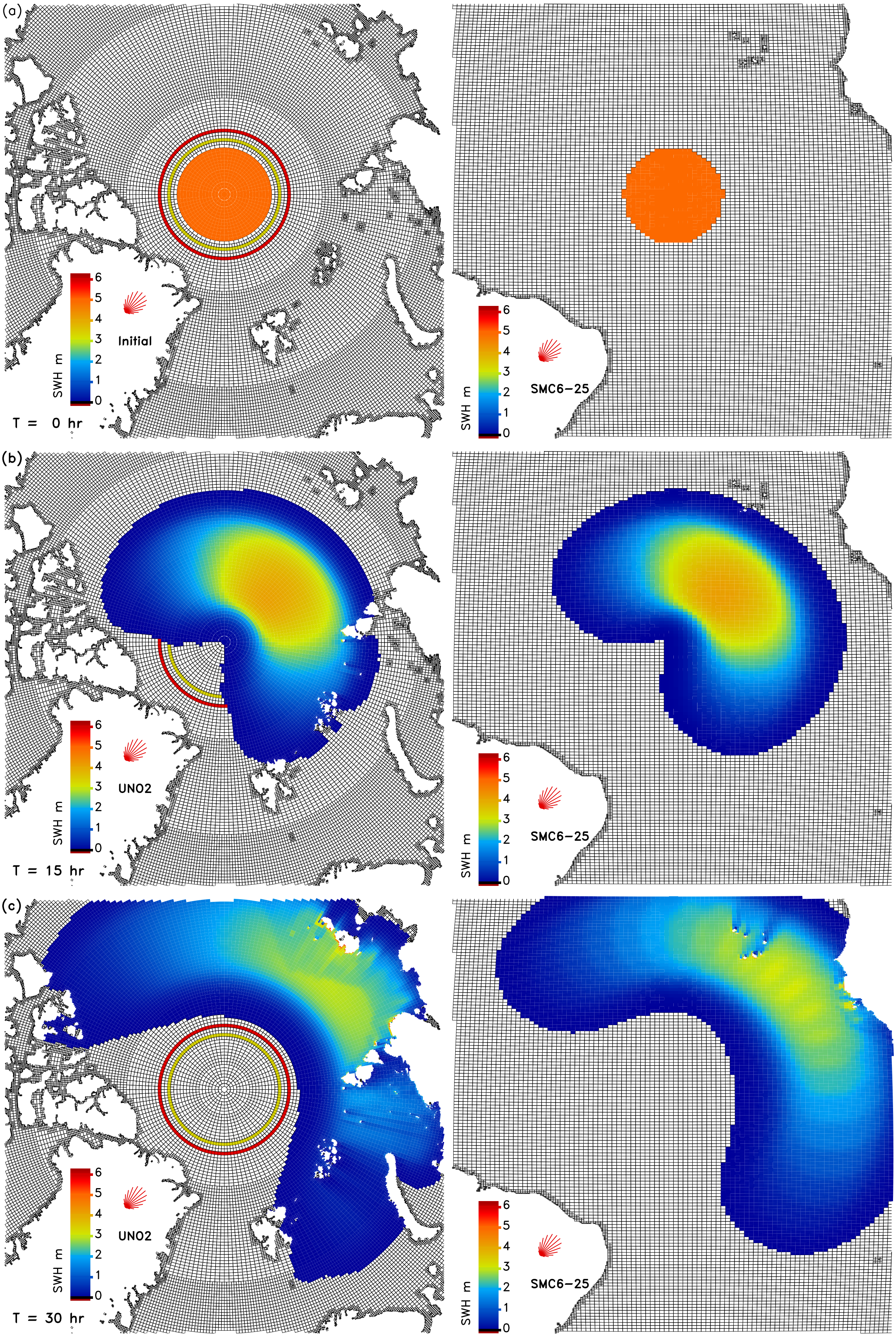

Fig.4. Comparison of the wave spectral propagation using Arctic map-east (left column) and the conversional local east (right column reference direction methods.

Because the polar region of the Arctic Ocean is still covered by sea ice, it is not practical to validate the map-east method against wave observations. Here a simple approach is used to assess the map-east method by comparing the propagation of the Arctic and Atlantic patches. As long as the two patches have similar propagation pattern, the map-east method may be considered to be equivalent to the local east method. The two round patches are drawn side-by-side in Fig.4 for this comparison. The global perspective of the two initial round patches are shown in row (a) of Fig.3 and the non-zero wave height is constant 5 units. Because of the different shapes of the grid cells at the two sites, the Arctic patch has a round edge while the Atlantic patch has a stepped edge. Nevertheless, the two patches cover approximately the same area.

The two co-centred rings in the Arctic plots mark the transient zone from the local east to the map-east reference directions. The initial spectral peak direction θ_p is 45º from their reference direction, respectively, as indicated by the spectral roses in Fig.4. Because the Arctic part uses a fixed map-east reference direction, the initial spectral peak direction is constant within the Arctic part. In the global part, however, the local east reference direction changes with longitude and so the peak direction of the initial spectrum. This is why the Atlantic round patch is initialised near the Equator to minimise the local direction change.

The middle row (b) of Fig.4 shows the two patches after 15 hrs of propagation. The centre of the Arctic patch has covered the transient zone. It is evident that there is no visible interruption of the patch distribution in the two reference direction parts. The Arctic patch is quite similar to the Atlantic one shown on the right side except for the fine cuttings caused by local islands. The bottom row (c) of Fig.4 shows the two patches after 30 hrs when the Arctic patch is out of the map-east zone. The two patches still share a quite close distribution in the deep waters. The blocking effects by local islands and water depth induced refraction and speed changes have left their unique marks on the two patches. These results confirm that the map-east method is effective for wave spectral propagation in the polar region and solved the polar problem in finite difference schemes on reduced grids. The transition between the two reference direction zones is smooth and does not cause any visible interruptions in surface wave spectral propagation.

6. Example SMC grids

In addition to the global SMC6-25 grid discussion in previous sections, here a few more SMC grids are included to illustrate the flexibilities of the SMC grid.

i) SMC6125 Global-UK grid

This is a slight variation of the global SMC6-25 grid by increasing the resolution around the UK waters to a minimum of 12 km cells. A portion of the SMC6125 grid around the UK waters is shown in Fig.5.

ii) Atlantic SMC6-25 grid

The Atlantic SMC6-25 grid shown in Fig.6 is a regional selection of the global SMC6-25 cells over the Atlantic Ocean. Thanks to its unstructured nature of the SMC grid, a portion of the global cells can be regrouped to form a regional model. To minimise boundary input, the selected Atlantic domain follows coastlines all the way from the Antarctic to Arctic except for a few short cross-sections, particularly the two over the Sothern Ocean, between the Cape Horn in S America 69W) and Cape Agulhas (20E) at the tip of S Africa. The Atlantic domain is retuned to remove unimportant branches at the outskirts, such as the Gulf of Mexico, the Hudson Bay, and the Mediterranean. Fig.6 shows the selected Atlantic SMC6-25 grid. The base resolution is at 25 km with refined 12km and 6km cells near coastlines.

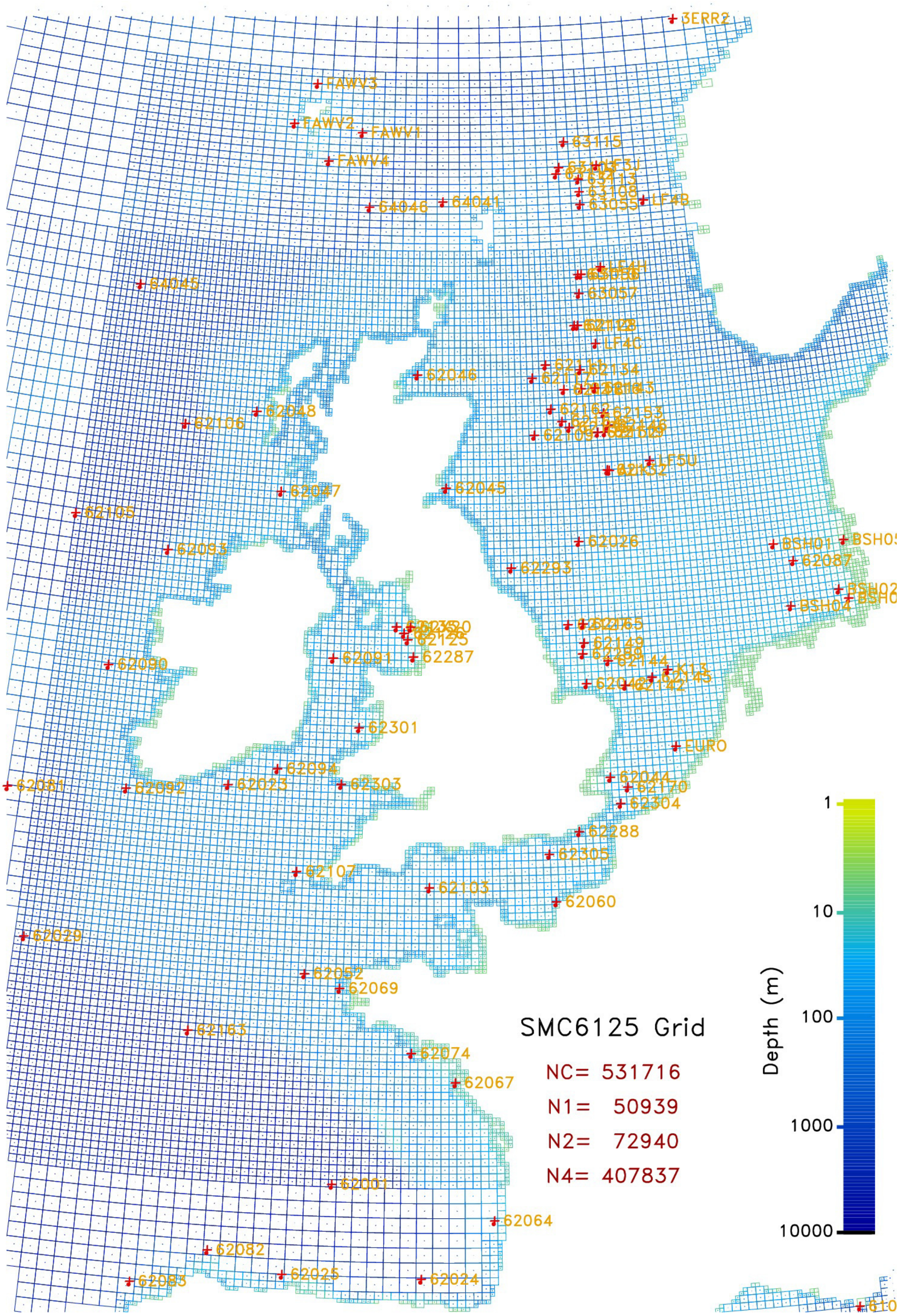

Fig.5. The SMC6125 grid around the UK waters.

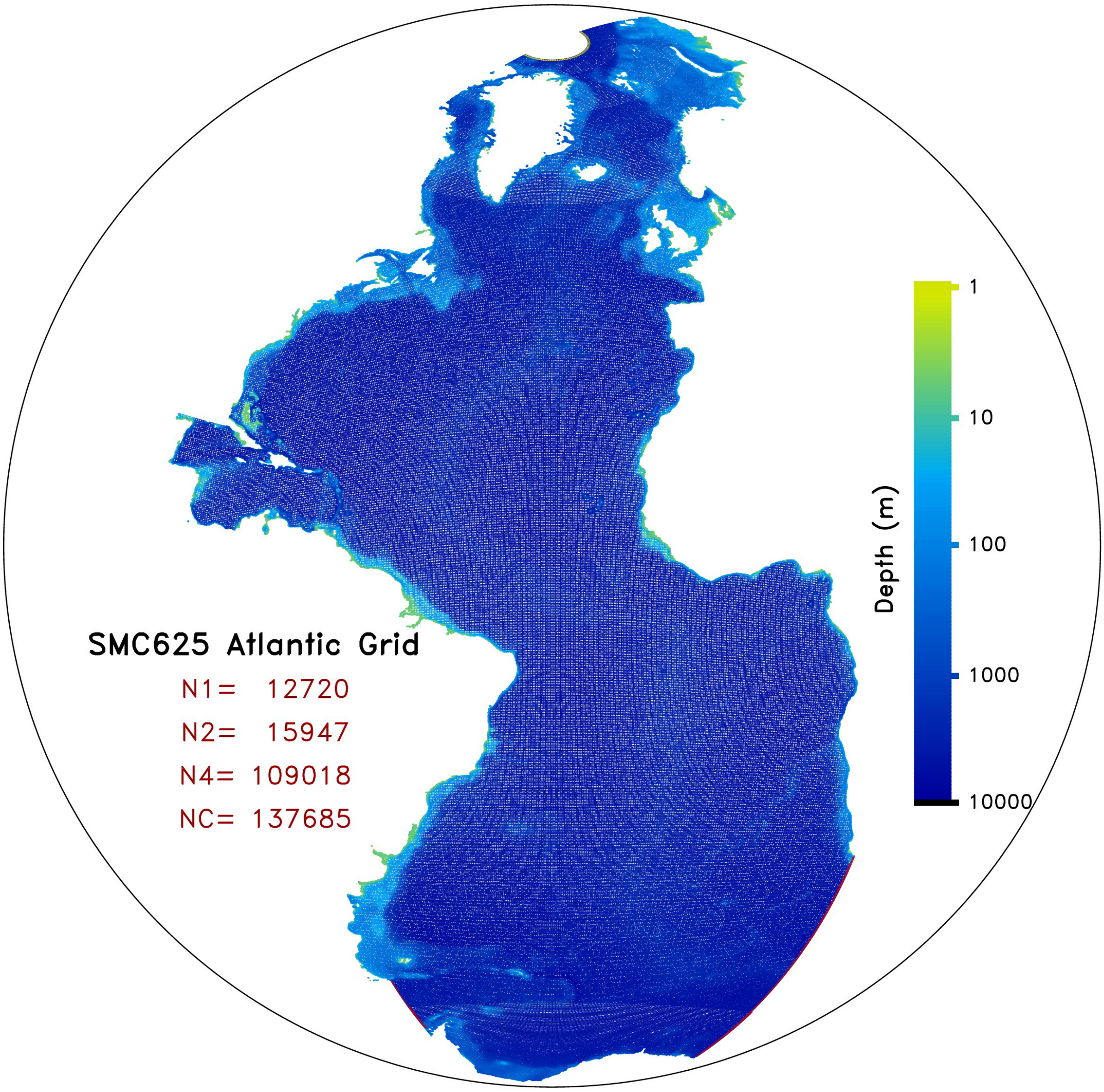

Fig. 6. The Atlantic SMC grid for ocean surface wave model.

Only the two cross-sections in the Southern Ocean will be fed with boundary conditions for the Atlantic model. Boundary conditions at Strait of Gibraltar, Baltic Sea, Gulf of Mexico (La Habana - Miami), Hudson Bay, and Baffin Bay are ignored as they are either quite small or sheltered by nearby islands.

In WW3, boundary conditions are applied by defining grid points with boundary data and these points do not need to be on the outside of the grid. The boundary cells are defined in the SMC grid by an additional boundary cell input file. The boundary data for the Atlantic model are generated by a regular grid wave model with identical spectral resolution.

iii) The Great Lakes SMC0512 grid

This is a regional model to cover the Great Lakes at variable resolution from 0.5km to 2 km. As the Great Lakes are isolated from the oceans, this model domain does not need any boundary conditions. Also note the SW corner of the corresponding regular grid at 2km resolution is chosen as the SMC grid index reference point so the index shifting numbers for the SMC0512 grid becomes zero.

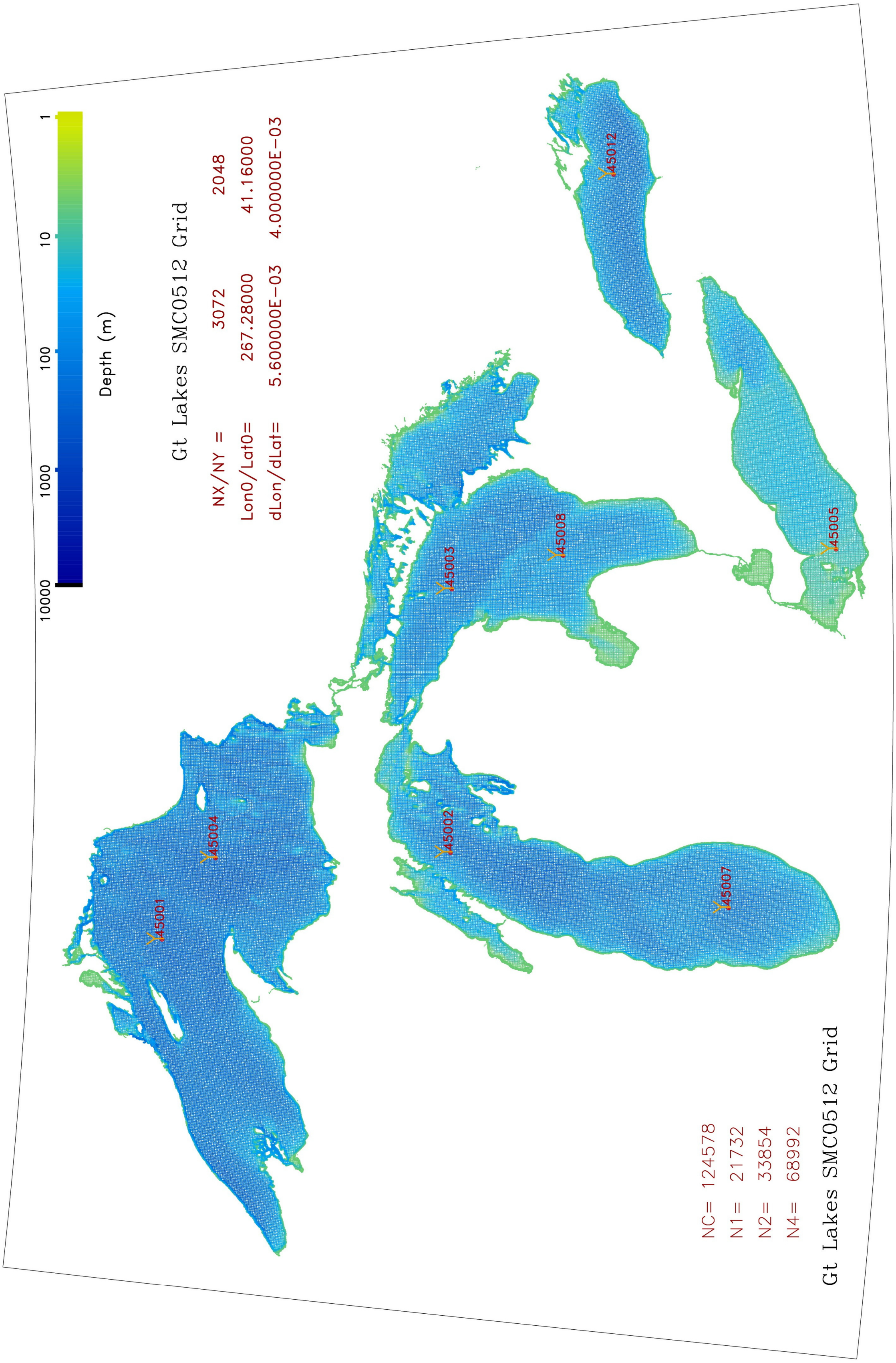

Fig.7. The SMC0512 grid for the Great Lakes.

iv) The SMC50km grid

This is a sample grid, users may try to generate it from files provided in the WW3 model package, particular in smc_docs/SMC_TKs/. Fig.8 illustrate the Arctic region of this global grid to highlight the selection of the Arctic part to run a full global model.

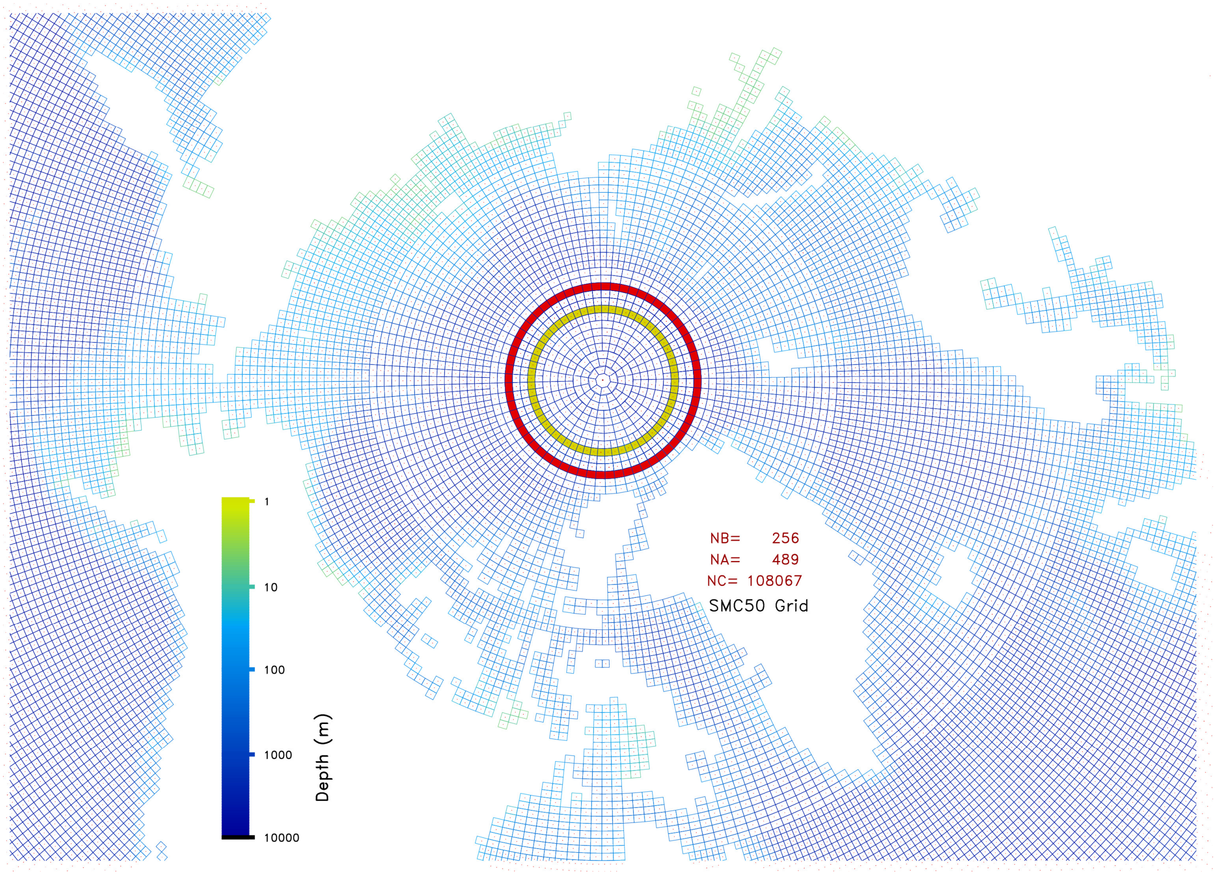

Fig.8. The Arctic region of the SMC50km grid to illustrate the Arctic part selection.

Following the following steps to generate the SMC50km grid and run the wave model WW3 V5.18, plus some sample visualization.

1) To generate the SMC50km cell arrays, run the idl program
`smc_docs/SMCG_TKs/Glob50SMCels.pro`,
which will read the bathymetry data
`smc_docs/SMCG_TKs/G50kmBathy.dat`
and produce the global cell array file, `G50SMCelsA.dat`, including the Arctic.

2) Decide how large the Arctic part you like and divide the `G50SMCelsA.dat` into the global and Arctic parts. I chose all cells above ~ 84ºN or j >= 179. Note that there are 4-overlapping rows between the global and Arctic part so the global part actually contains all cells upto j = 182.

3) Sort the global part cells with `smc_docs/SMCG_TKs/countcells`
The Arctic part is already in the right order so there is no need to sort it but the first count line has to be entered manually by counting the total number of cells in the Arctic part and the boundary cells for the first two and next two overlapping rows. In my example file `G50SMCBAr.dat` the first count line is

```
  489  128  128
```

3b) You may now visualize the SMC50km cells with an idl script
`smc_docs/SMCG_TKs/g50smcgrids.pro`
which has some tuneable parameters to choose your view point and area. The projection will be saved in 3 data files, which can be used later for wave output visualization (from the same view point).

4) Generate face arrays with `smc_docs/SMCG_TKs/G50SGlSide.f90` and `G50SAcSide.f90` for the global and Arctic part, respectively. They will read the sorted cell arrays as input.

5) Sort the face arrays (output from `G50SGlSide.f90` and `G50SAcSide.f90`) with `smc_docs/SMCG_TKs/countijsd.`

6) Generate the subgrid obstruction ratio with
`smc_docs/SMCG_TKs/Glob50SMCObstr.pro`
which will read the subgrid obstruction data (on full grid)
`smc_docs/SMCG_TKs/G50kmObstr.dat`
and produce a SMC cell only sub-grid obstruction file `G50GObstr.dat`, plus a text information file for setting up the regular grid input files (wind, ice, etc if any).

7) Prepare the model input files. Here are the list of files used in inp/

```
    23932 Nov 18  2013 G50AISide.dat
    29276 Nov 18  2013 G50AJSide.dat
  5356170 Oct 20  2014 G50GISide.dat
  5792134 Oct 20  2014 G50GJSide.dat
   537907 Oct 20  2014 G50GObstr.dat
    13223 Oct 20  2014 G50SMCBAr.dat
  2904635 Oct 20  2014 G50SMCels.dat
    26530 Apr 13 15:50 ww3_grid.inp
     3146 Apr  5 10:55 ww3_outf.inp.template
     7097 Oct  4  2013 ww3_outp.inp.template
     8770 Apr  5 13:50 ww3_shel.inp.template
     3401 Dec 20  2012 ww3_strt.inp
```

Note the `*.inp.template` files require substituting the model start/end times to generate the final `*.inp` files.

8) Prepare the forcing wind, ice and current files if any. These forcing files remain the same as on a regular lat-lon grid. The corresponding regular grid settings are available from the `inp/ww3_grid.inp`.

9) Compile the WW3 model with the following switch file
`smc_docs/SMCG_TKs/switch`
Note that this is for series executables. For parallel ones swap '`SHRD`' with '`DIST MPI`' in the switch file.

10) Run the `ww3_grid` program to generate the `inp/mod_def.ww3` file

11) Run the `ww3_shel` with all input files to generate wave model output.

12) Post-processing from `out_grd.ww3`, depending on which format you like. I use the full text output converted by `ww3_outf (type 4)` and then visualized with the idl program `smc_docs/SMCG_TKs/g50smcswhglb.pro`, which will use the same projection as saved in step (3b) for the SMC50km cell visualization.

Enjoy your wave modelling with the SMC grid and contact me if you need any help.

References

Booij, N., L.H. Holthuijsen, Propagation of ocean waves in discrete spectral wave models, *J. Comput.* Phys. **68** (1987) 307-326.

Booij, N., R.C. Ris, L.H. Holthuijsen, A third-generation wave model for coastal regions, 1. Model description and validation, *J. Geophys. Res*. **104** C4 (1999) 7649-7666.

Chawla, A., H.L. Tolman, Obstruction grids for spectral wave models, *Ocean Modelling* **22** (2008) 12-25.

Falnes, J., *Ocean Waves and Oscillating Systems*. Cambridge University Press, Cambridge, UK, 2002, 275pp.

Hardy, T.A., L.B. Mason, J.D. McConochie, A wave model for the Great Barrier Reef, *Ocean Engineering*, **28** (2000) 45-70.

Leonard, B. P., A.P. Lock, M.K. MacVean 1996: Conservative explicit unrestricted-time-step multidimensional constancy-preserving advection schemes. *Mon. Wea. Rev*., **124**, 2588-2606.

Li, J.G., Upstream non-oscillatory advection schemes, *Mon. Wea. Rev*., **136** (2008) 4709-4729.

Li, J.G., Global transport on a spherical multiple-cell grid, *Mon. Wea. Rev*., **139** (2011) 1536-1555.

Li, J.G., Propagation of Ocean Surface Waves on a Spherical Multiple-Cell Grid, *J. Comput. Phys*., **231** (2012) 8262-8277.

Phillips, O.M., *The Dynamics of the Upper Ocean*, 2nd Ed., Cambridge Univ. Press, Cambridge, UK, 1977, 336pp.

Rasch, P.J., Conservative shape-preserving two-dimensional transport on a spherical reduced grid. *Mon. Wea. Rev*. **122** (1994) 1337-1350.

Roe, P.L., Large scale computations in fluid mechanics, in: E. Engquist, S. Osher, R.J.C. Sommerville (Eds.), *Lectures in Applied Mathematics*, **22** (1985) 163-193.

Tolman, H.L., A third-generation model for wind waves on slowly varying unsteady and inhomogeneous depths and currents. *J. Phys. Oceanogr*. **21** (1991) 782-792.

Tolman, H.L., Alleviating the Garden Sprinkler Effect in wind wave models, *Ocean Modelling*, **4** (2002) 269-289.

Tolman, H.L., Treatment of unresolved islands and ice in wind wave models, *Ocean Modelling*, **5** (2003) 219-231.

Tolman, H.L., A mosaic approach to wind wave modeling. Ocean Modelling, **25** (2008) 35-47.

Tolman, H.L., B. Balasubramaniyan, L.D. Burroughs, D.V. Chalikov, Y.Y. Chao, H.S. Chen, V.M. Gerald, Development and implementation of wind-generated ocean surface wave models at NCEP, *Weather and Forecasting,* **17** (2002) 311-333.

WAMDI group, The WAM model - a third generation ocean wave prediction model, *J. Phys. Oceanogr*. **18** (1988) 1775-1810.

WISE Group, L. Cavaleri, J.-H.G.M. Alves, F. Ardhuin, A. Babanin, M. Banner, K. Belibassakis, M. Benoit, M Donelan, J. Groeneweg, T.H.C. Herbers, P. Hwang, P.A.E.M. Janssen, T. Janssen, I.V. Lavrenov, R. Magne, J. Monbaliu, M. Onorato, V. Polnikov, D. Resio, W.E. Rogers, A. Sheremet, J. McKee Smith, H.L. Tolman, G. van Vledder, J. Wolf, I. Young, Wave modelling - the state of the art. *Progress Oceanogr.* **75** (2007) 603-674.